1 OF 1

1-24416

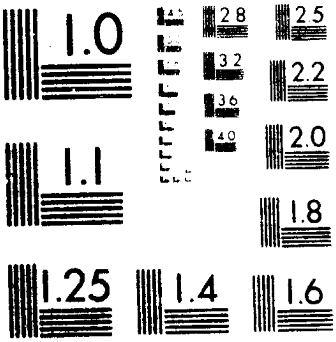

MICROCOPY RESOLUTION TEST CHART

NATIONAL BUREAU OF STANDARDS

(NASA-TM-83109) COMBINED SINGLE-PULSE HOLOGRAPHY AND TIME-RESOLVED LASER SCHLIEREN FOR FLOW VISUALIZATION (NASA) 16 p

N81-24416

HC A02/MF A01 CSCL 14E

Unclas

G3/35 25029

NASA Technical Memorandum 83109

Combined Single-Pulse Holography and Time-Resolved Laser Schlieren for Flow Visualization

A. W. Burner and W. K. Goad
Langley Research Center
Hampton, Virginia

NASA
National Aeronautics
and Space Administration

Scientific and Technical
Information Branch

1981

SUMMARY

A pulsed ruby laser and continuous-wave argon ion laser have been used in a combined setup at the Langley Expansion Tube for single-pulse holography and time-resolved laser schlieren with a common optical axis. The two systems can be operated simultaneously for a single run. For a single frame, the pulsed holographic setup offers the options of shadowgraph, schlieren, and interferometry from the reconstructed hologram as well as the advantage of post-run sensitivity adjustments. For flow-establishment studies the time-resolved laser schlieren provides visualization of the flow field every 12.5 μs for up to 80 frames with an exposure time per frame of 5.4 μs.

INTRODUCTION

For many tests at the Langley Expansion Tube, a single flow visualization record taken during the 200 to 300 μs run is sufficient. In the past (ref. 1) a white-light schlieren system was used for this single flow visualization record. The single-record system was replaced recently (ref. 2) by a holographic recording system which has several advantages over nonholographic techniques for flow visualization. Light emitted by shock-heated gas about a blunt body is incoherent with the laser light used for the holographic recording and thus is not visible in the holographic reconstruction (although a decrease in hologram diffraction efficiency can occur). This light emitted by the shock-heated gas can reduce the ability to accurately define shock locations in nonholographic flow visualization, even when high-speed capping shutters are used (ref. 1). The holographic system has also proven to be more reliable, allows for post-run sensitivity adjustments, and offers the additional capability of interferometry with little extra effort over the schlieren system. With interferometry, the density flow field can be either computed directly for 2-D or axisymmetric flows, or mathematical flow models can be verified by comparing predicted to measured fringe shifts.

Although an accurate shock-shape measurement can be made from a single record, it is often desirable to have a record of the flow as a function of time to study flow establishment (ref. 3). This requirement was met in the past by recording white-light schlieren with a high-speed framing camera (ref. 4). For a recent series of tests at the Expansion Tube, time-resolved flow visualization was required without giving up the advantages of holographic recording. Both of these requirements were accomplished by using a high-speed framing camera to record laser schlieren at a different wavelength than the holographic system so that the laser schlieren and holographic systems could be used together for a single run. Since the laser source size is much smaller than conventional white-light schlieren sources, the laser schlieren has increased sensitivity which is especially important due to the low free-stream densities in the expansion tube. The combined use of the two systems is discussed and examples of simultaneous flow visualization from the two systems are presented.

Use of trade names or names of manufacturers in this report does not constitute an official endorsement of such products or manufacturers, either expressed or implied, by the National Aeronautics and Space Administration.

EXPANSION TUBE DESCRIPTION

The Langley Expansion Tube (ref. 1) is a hypersonic, hypervelocity facility used for real-gas studies (ref. 5). The facility consists of a cylindrical tube with an internal diameter of 15.24 cm containing a driver or high-pressure chamber, an intermediate chamber which is evacuated and filled with the desired test gas, and an expansion or acceleration chamber. A high-pressure, double-diaphragm apparatus separates the driver and intermediate chambers. A low-pressure, secondary diaphragm separates the intermediate and expansion chambers. This secondary diaphragm can be removed to operate the facility as a conventional shock tube. The pressures in the chambers are adjusted to give the desired simulated environment.

Upon rupture of the double diaphragm, the high-pressure driver gas pushes a shock wave through the test gas contained in the intermediate chamber, thereby heating the gas. This shock encounters and bursts the weak secondary diaphragm, resulting in a secondary wave that travels through the acceleration gas and is followed by the test gas. Hence, the model is first subjected to the very low density acceleration gas followed by the test gas (fig. 1). Test gases generally used are air, He, N_2, Ar, Ne, CO_2, and mixtures such as H_2-He and N_2-CH_4. Free-stream densities in expansion tube mode are typically 5×10^{-3} kg/m^3 with density ratios across a normal shock ranging from 3.7 for He to 20 for CO^2. Free-stream velocities range from 5000 to 7000 m/s and free-stream Mach numbers range from 6 to 9.6. The flow about a model tested in the open-jet test section is observed through 8.2-cm-thick schlieren quality windows which have a 40 cm diameter clear aperture. Expansion tube run times are typically 200 to 300 us.

EXPERIMENTAL ARRANGEMENT AND RESULTS

The combined time-resolved laser schlieren and pulsed holographic flow visualization setup is shown in figure 2. The holographic system, which is described in reference 2, uses the Z-configuration common to off-axis schlieren systems. A ruby laser with a wavelength of 694 nm and pulse width of 20 ns is used as the source. For time-resolved laser schlieren, a continuous-wave argon ion laser was used as the light source to record a time history of the flow on a continuous-writing high-speed camera. Shutter times of less than 1 ms were required to prevent rewriting of the high-speed framing camera. Since such short exposures were not possible with an electronic shutter, an acousto-optical cell (AO cell) located outside the laser cavity was used for shuttering. The cell had a diffraction efficiency of 80 percent and an extinction ratio greater than 500 to 1. The extinction ratio could have been increased, but with increased light loss, by placing the cell inside the laser cavity. Since the angle of diffraction of the first-order beam from the AO cell varies with wavelength, the laser was operated single line at 515 nm with an output power of 2 W. For system alignment, the r-f drive was applied to the AO cell at a high repetition rate so that the first-order beam appeared continuous. The first-order diffracted beam from the AO cell was passed through a microscope objective and pinhole combination to be expanded and spatially filtered before passing through the hologram plate and illuminating the first parabolic mirror (40 cm diameter, 245 cm focal length). The parabolic mirror was tilted 5.8° so that the beam would be incident at right angles to the test section windows. An electronic capping shutter with an open time of 3 ms was placed after the AO cell to prevent light which passed through the cell, when switched off, from fogging the hologram. The AO cell was triggered by a delayed signal from an upstream wall gauge to produce a 0.8 ms pulse after the capping shutter was fully open. A photodiode detected a portion of the argon beam to record both the relative laser power and AO cell on-time on an oscilloscope. Kodak 120-02 holographic plates were used for hologram recording in the ruby laser system. The glass substrate of these plates was 1 mm thick. The 120-02 plates have reduced sensitivity in the green region of the spectrum so that the 0.8 ms argon laser pulse produces very little fog. Transmission of the 515 nm argon beam through an unexposed plate was measured to be 75 percent. Agfa 10E75 plates were not acceptable due to the high fog level from the argon laser exposure.

After collimation by the first parabolic mirror, the argon beam passes through the test section and is then refocused by the second parabolic mirror whose optical axis is parallel to the optical axis of the first parabolic mirror. Note that the argon beam has the same optical axis as the ruby beam but travels in the opposite direction. In reference 1 it was necessary to have the time-resolved system aligned slightly off axis to prevent interference with the single-frame system. Half of the argon beam is split with a 1-cm-thick dielectric-coated beam splitter before coming to a focus. The back surface of the beam splitter is antireflection coated and the beam splitter is wedged (30 min) so that no secondary fringes are seen. An interference filter which passed 90 percent of the ruby beam and reflected 90 percent of the argon beam was used initially as beam splitter, but a second surface reflection produced objectionable vertical fringes in the argon beam.

Aberrations are introduced into both the holographic and laser-schlieren systems by the hologram substrate. The beam splitter aberrates only the holographic system since the ruby beam passes through it, whereas the argon beam is reflected from its first coated surface. A ray trace determined that the minimum spot size at the best focus for both systems was less than that predicted by diffraction theory in the direction perpendicular to the knife-edge. The wedge and lack of surface flatness which varies from hologram plate to hologram plate did not appear to degrade the schlieren quality of either system.

After reflection from the beam splitter, the argon beam is directed to an adjustable knife-edge placed at the horizontal focus of the astigmatic beam. Knife-edge cutoff was set before each run for maximum sensitivy.

The high-speed framing camera (fig. 3) used for these tests was 141 cm long by 85 cm wide by 182 cm high with a mass of 4000 kg. Even though the design for this camera is 20 years old, it is still unsurpassed when both large numbers of frames and extremely high framing rates are required. A first-order optical layout of the camera is shown in figure 4. An objective lens with a focal length of 61 cm images the event onto a three-surface mirror which is made to rotate at high speeds by a gas turbine. One revolution of the mirror causes the image to sweep around the camera three times. The rate of revolution is monitored on a counter connected to an electromagnetic pickup. Since there are 80 frames, the time between frames is T/240 where T is the period for one revolution of the three-surface mirror. The exposure time per frame is dependent on the internal stops and is T/556 (ref. 6). If compressed helium is used to drive the rotating mirror, the time between frames can be as short as 0.7 us with a frame exposure time of 0.3 us. For this series of tests, compressed air was used to drive the rotating mirror. Typical periods were 3 ms corresponding to a time between frames of 12.5 us and frame exposure of 5.4 us. The time between frames for a given run was determined by dividing the argon laser on-time by the number of exposed frames. If the on-time is known to 10 us, then the time between frames can be determined to better than 0.17 us (for 800 us on-time and 60 frames). The time between the end of one frame and the beginning of the next frame is typically 7 us. This value is assumed to be the uncertainty in determining the start of shock formation about the model.

The camera has an effective f-number of 26. The three surfaces of the rotating mirror are spherically concave to image the entrance stops located slightly behind the objective lens onto the exit stops of the camera which increases the field of view. Relay lenses inside the camera reimage the scene onto two 35 mm format stationary film strips located on the top and bottom of the camera. The two entrance stops are diamond shaped and displaced vertically. Image forming rays which pass through the top and bottom stops are imaged onto the top and bottom film strips, respectively. Rays from any point of a diffuse object pass through both stops so that a complete image is formed at any one time on either the top or bottom film strip depending upon the position of the three-surface mirror.

In a schlieren system the imagery consists of both the undeviated light beam and diffracted light from the flow field and surface of the model. The most straightforward way to get an acceptable schlieren image on the film plane of such a camera is to project the schlieren image onto a ground glass focusing screen which can then be imaged with the objective lens of the camera. The light loss introduced by the focusing screen makes such an approach unacceptable, making it necessary to have the camera accept the nondiffuse light directly by splitting the schlieren beam and directing the two beams through the two entrance stops. This was accomplished in an earlier white-light schlieren setup using the same camera (ref. 4) by splitting the schlieren beam at its focus with a mirrored prism beam splitter which also acted as a knife-edge. The prism beam splitter causes the sensitivity to be fixed and the shock images from the two entrance stops to be of opposite contrast. The prism beam splitter was found to be unusable with the laser source due to the much smaller source size of the laser, and hence increased sensitivity. Therefore, a beam splitter and mirror arrangement was placed directly in front of the camera to split the schlieren beam into two parallel beams which then passed through the two entrance stops. With the beam splitter and mirror arrangement the sensitivity is variable and the image contrast through both entrance stops is the same.

A 7-cm-diameter telescope doublet with a focal length of 76 cm reimaged the horizontal schlieren focus through the entrance stops without vignetting. A 3.8-cm-diameter biconvex lens with a focal length of 2 m was placed at the reimaged vertical focus in front of the objective lens of the camera to cause the center of the test section to appear to be at infinity to the camera. The camera had a relatively large depth of field but small depth of focus. The short exposure time per frame required the use of a very high sensitivity film, Kodak high-speed type 2485. A development time of 2.5 min at 35°C in 857 developer provided sufficient image density for shock detection without serious loss of image quality due to graininess.

The spatial resolution in the object plane for both the holographic and laser-schlieren systems was determined experimentally by recording the image of a variable frequency test chart placed at the center of the test section. The spatial resolution of the holographic system was measured to be better than 13 lines/mm in the object plane whereas the time-resolved laser-schlieren system had a spatial resolution of less than 4 lines/mm at the object. The difference in magnification between the horizontal and vertical directions on the image was measured to be 1 percent for the holographic system and 1.5 percent for the time-resolved laser schlieren.

The combined use of the two systems for a single run enables the aerodynamicist to study flow establishment about test models with time-resolved laser schlieren and to obtain excellent shock-shape measurements for a single frame from the holographic recording. The study of flow establishment is necessary at the Expansion Tube to determine the time required to establish quasi-steady flow about a model. Results from flow-establishment studies made in shock tubes can serve as a guide, but are not directly applicable to the Expansion Tube since the operating sequence (fig. 1) differs in that the test model is subjected to the acceleration-gas flow prior to the test-gas flow (ref. 3). Recordings made during a single run by the two systems for a sharp-leading-edge flat plate with 18° flap are shown in figures 5 (time history) and 6 (single frame). The test gas was air with a free-stream density of 6.2×10^{-3} kg/m^3 and free-stream velocity of 5360 m/s (Mach 7.5). The normal shock density ratio, an important parameter in the study of real-gas effects (ref. 5), was 11.2. The sequential frames of figure 5 are separated by 12.8 us with an exposure time per frame of 5.5 us. The knife-edge was horizontal and the cutoff was from below the schlieren focus. The schlieren image did not appreciably change from the sixth frame to the last frame of the recording. The corresponding hologram was exposed 145 us after the start of flow. Several different flow-visualization reconstructions from the single hologram are presented in figure 6. For a comparison of the present setup to that described in reference 1, several frames of schlieren which were made using the same high-speed camera with a white-light source are presented in figure 7 (taken from ref. 7). The test gas was argon with a free-stream velocity of 5320 m/s (Mach 8.7). Note the overexposure near the leading edge of the model due to light emitted by the shock-heated gas. This light is not troublesome for the holographic recording since the light is incoherent with the laser light used for recording the hologram and is not visible when reconstructing the hologram. Holographic recording of the flow field is especially advantageous for blunt bodies run in the expansion tube since the overexposure due to the shock-heated gas is even more pronounced for a blunt body than for a sharp-leading-edge model as presented here. For test conditions where the light emitted by the shock-heated gas is visible on the laser schlieren, a narrow bandpass interference filter centered on the laser wavelength can be used to filter out most of the nonlaser light.

CONCLUDING REMARKS

Laser schlieren using a continuous-wave argon ion laser and high-speed framing camera has been used simultaneously with a pulsed ruby laser holographic recording system to obtain both time-resolved laser schlieren for flow-establishment studies and a single-frame hologram from which accurate shock shapes can be obtained. The combined setup has proven to be reliable and has produced good data for a number of runs at the Langley Expansion Tube.

Langley Research Center
National Aeronautics and Space Administration
Hampton, VA 23665
May 15, 1981

REFERENCES

1. Moore, John A.: Description and Initial Operating Performance of the Langley 6-Inch Expansion Tube Using Heated Helium Driver Gas. NASA TM X-3240, 1975.

2. Burner, A. W.; and Goad, W. K.: Holographic Flow Visualization at NASA Langley. Instrumentation in the Aerospace Industry - Volume 25. Advances in Test Measurement - Volume 16, Part Two, Instrum. Soc. America, c.1979, pp. 477-484.

3. Miller, Charles G.; and Moore, John A.: Flow-Establishment Times for Blunt Bodies in an Expansion Tube. AIAA J., vol. 13, no. 12, Dec. 1975, pp. 1676-1678.

4. Mauldin, Lemuel E., III; and Compton, E. Conrad: An Optical System for Recording Schlieren Images With a Continuous-Writing Ultra-High-Speed Framing Camera. NASA TN D-4986, 1969.

5. Miller, Charles G., III: Shock Shapes on Blunt Bodies in Hypersonic-Hypervelocity Helium, Air, and CO_2 Flows, and Calibration Results in Langley 6-Inch Expansion Tube. NASA TN D-7800, 1975.

6. Operating Manual - Model 192 Framing Camera. Eng. Dept. 192-2-62, Beckman & Whitley, Inc.

7. Miller, Charles G.: Operational Experience in the Langley Expansion Tube With Various Test Gases. NASA TM-78637, 1977.

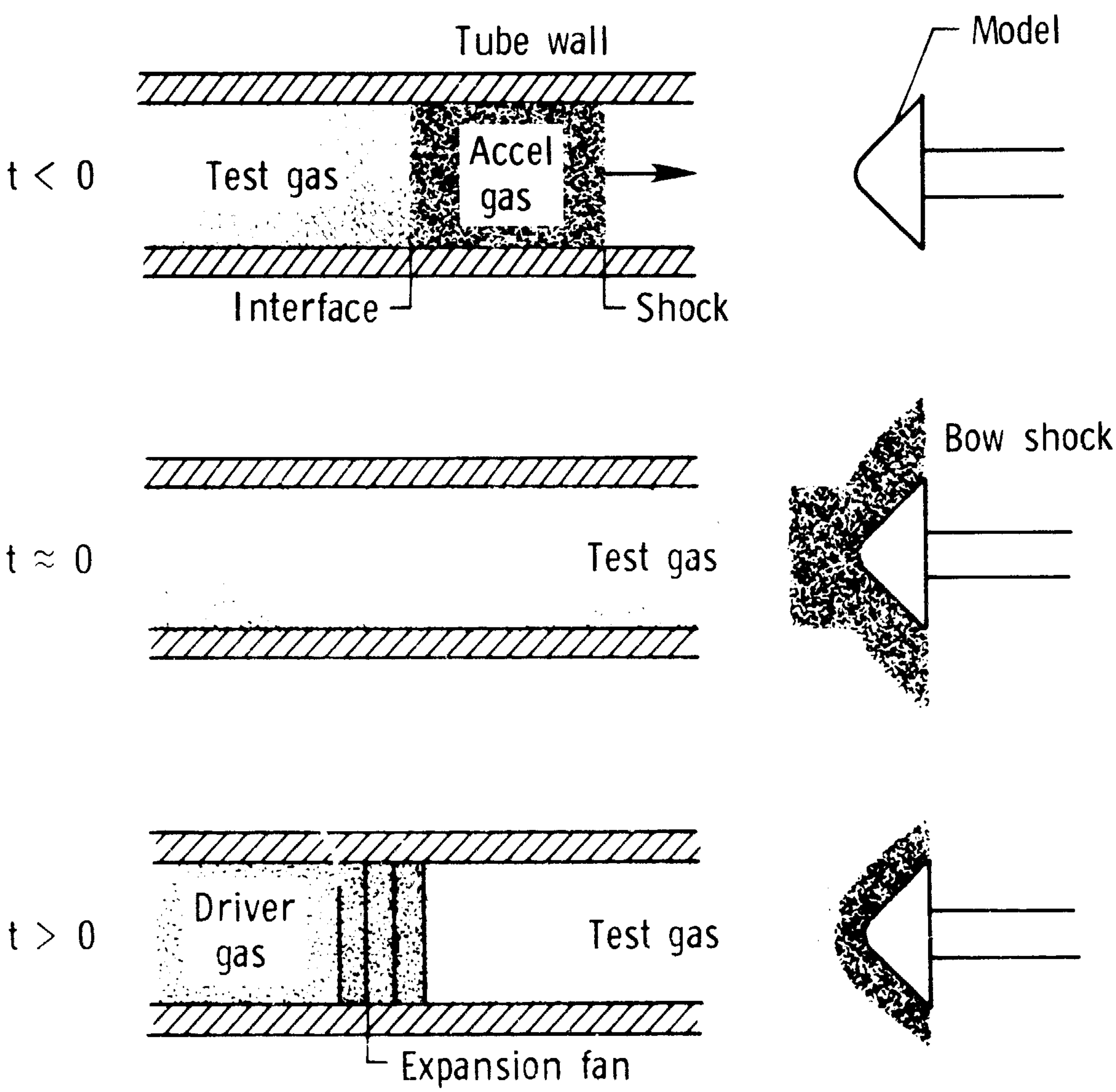

Figure 1.- Operating sequence of the Expansion Tube.
t = Run time.

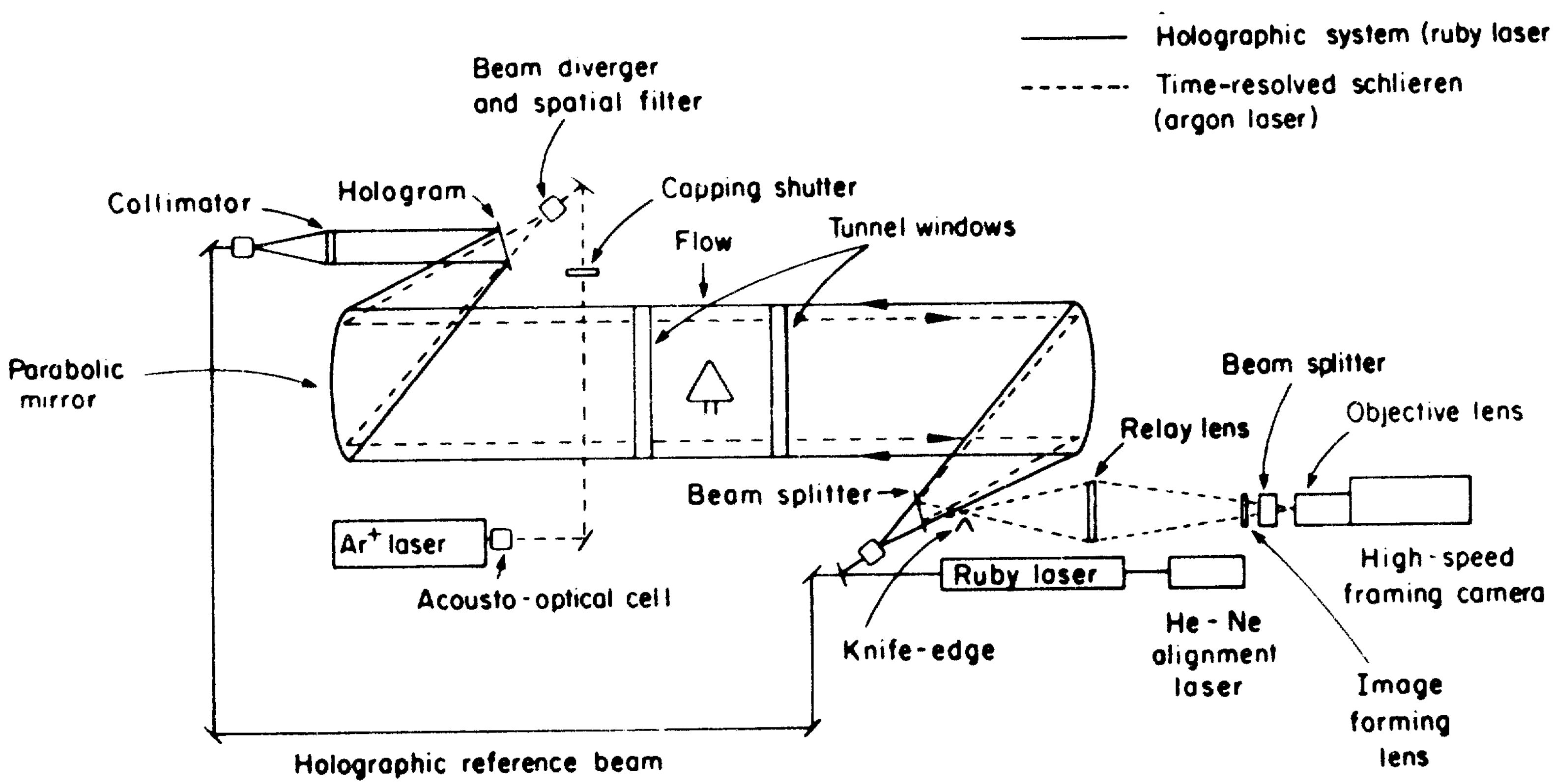

Figure 2.- Schematic of combined time-resolved laser schlieren and pulsed holographic flow visualization.

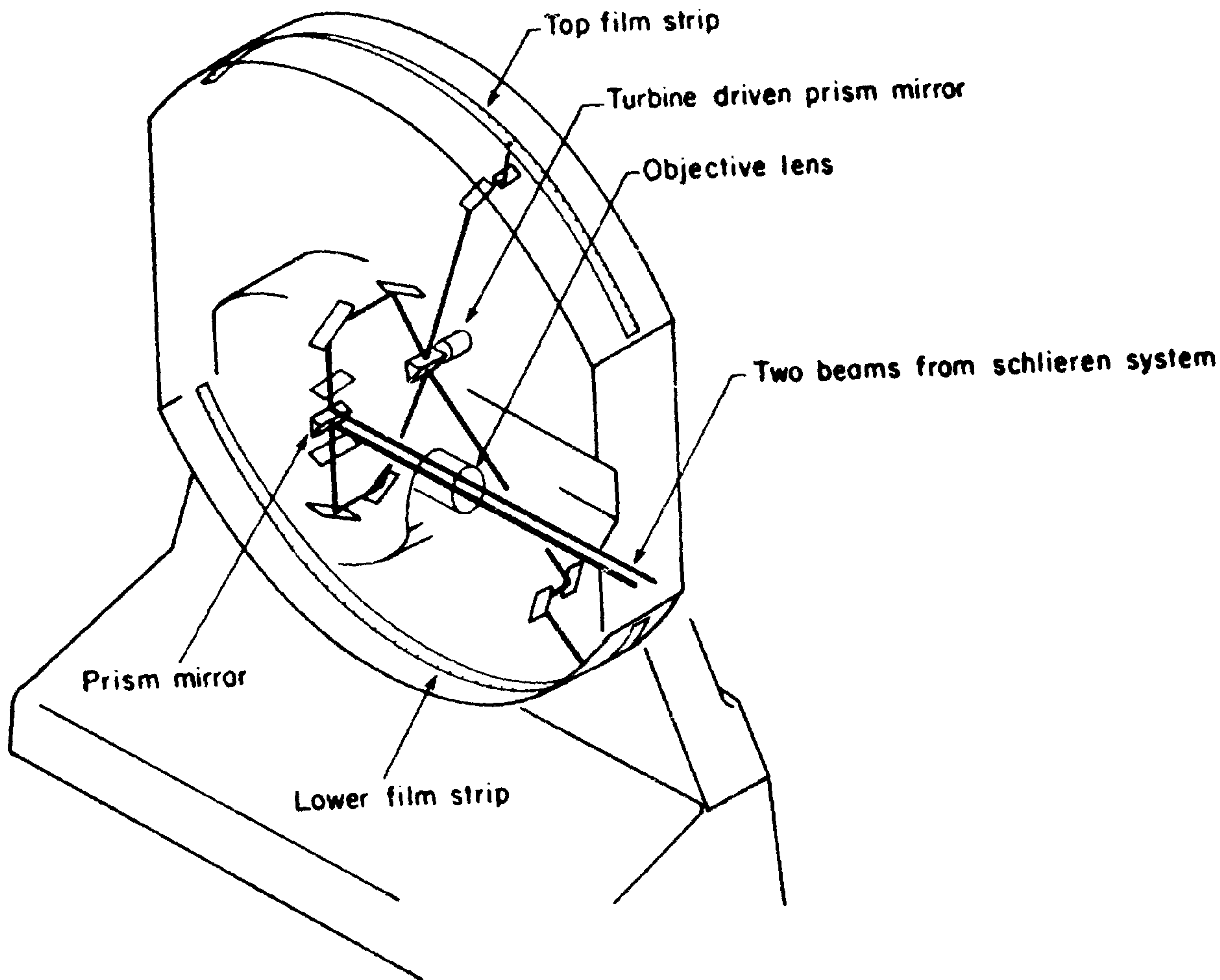

Figure 3.- Simplified schematic of high-speed framing camera (from ref. 6).

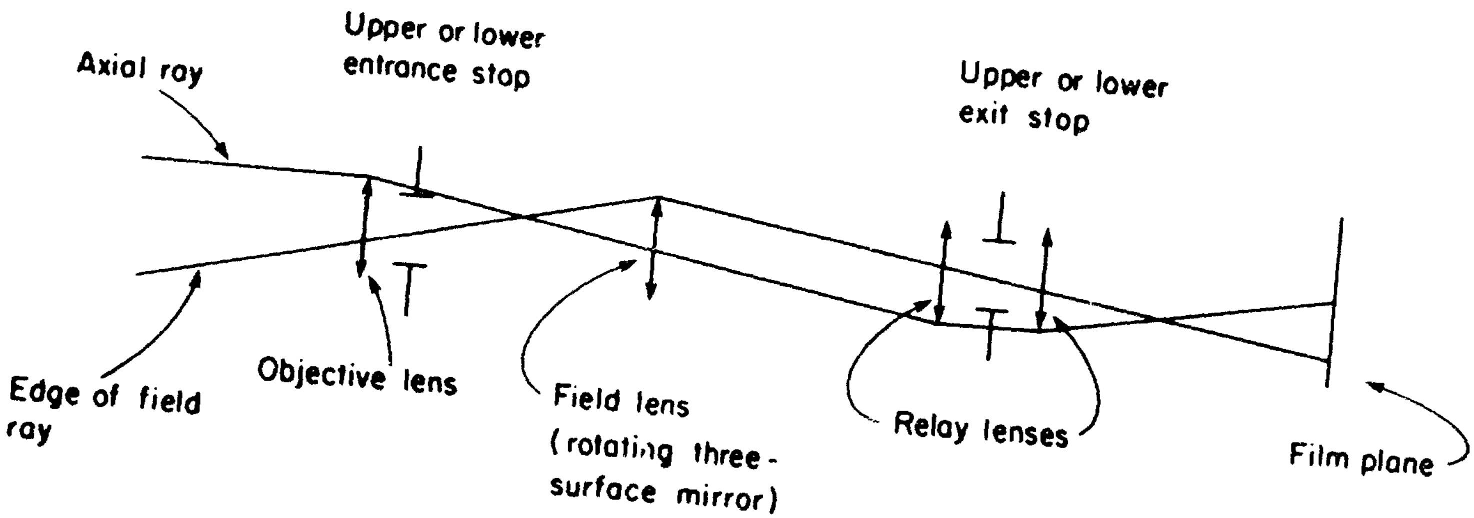

Figure 4.- First-order layout of high-speed framing camera.

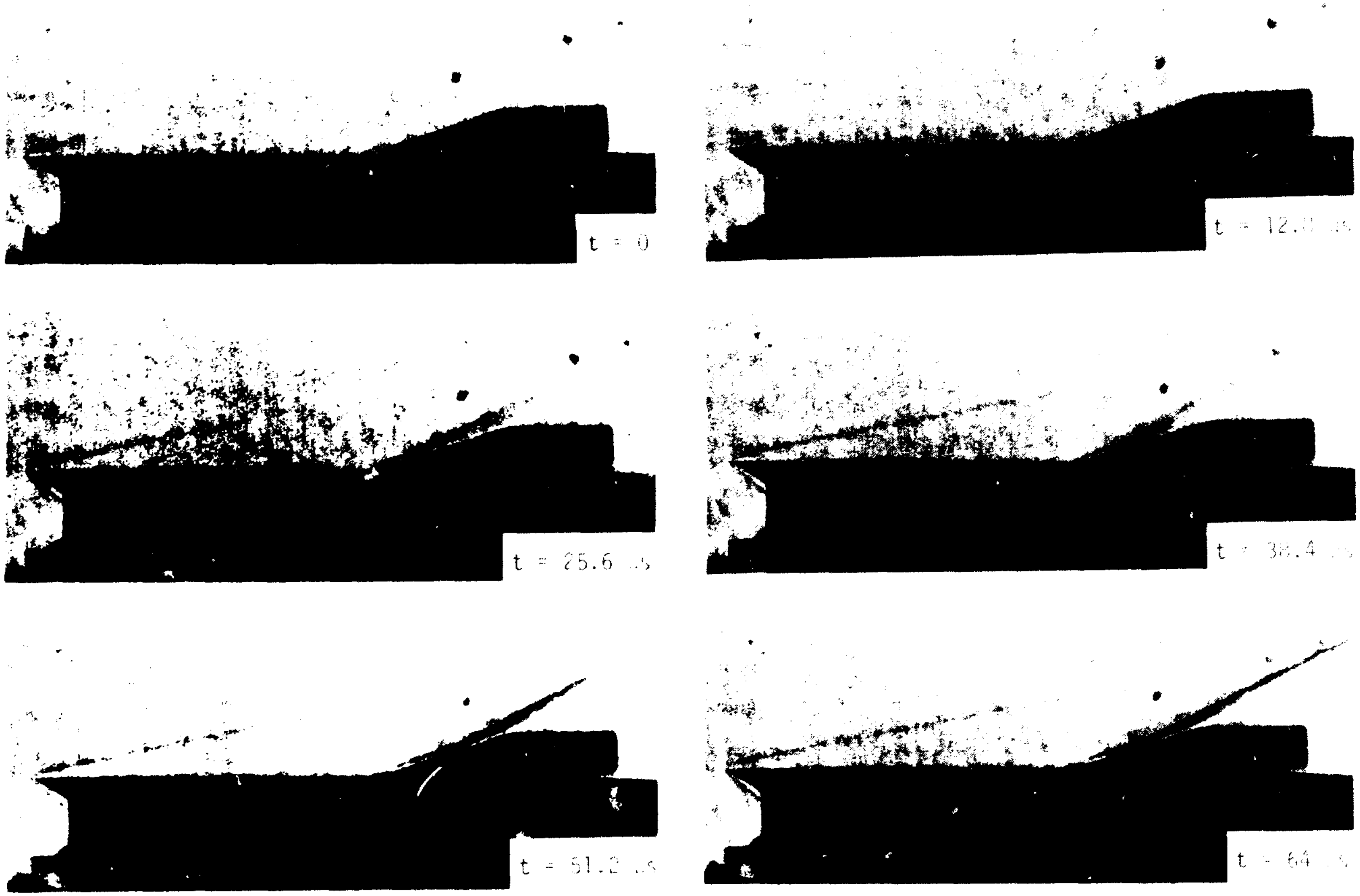

L-81-138

Figure 5.- Laser-schlieren sequential frames of sharp-leading-edge flat plate with 18° flap at Mach 7.5 in air. t = Run time.

(a) Focused shadowgraph.

(b) Defocused shadowgraph.

(c) Schlieren with horizontal knife-edge from top.

(d) Schlieren with horizontal knife-edge from bottom.

L-81-139

Figure 6.- Examples of flow visualization reconstructed from single hologram made during same run as figure 5.